Dwelltime Analysis of Symmetry-Breaking Dynamical Systems *

J. Vollmer [1], J. Peinke [2], and A. Okniński [3]

[1] Institute of Physics, University of Basel, CH-4056 Basel
[2] Physical Institute, University of Bayreuth, D-95440 Bayreuth
[3] Physics Division, University of Technology, P-25-314 Kielce

Z. Naturforsch. **50a**, 1117–1122 (1995); received August 4, 1995

Dwelltime analysis is known to characterize saddles giving rise to chaotic scattering. In the present paper it is used to characterize the dependence on initial conditions of the attractor approached by a trajectory in dissipative systems described by one-dimensional, noninvertible mappings which show symmetry breaking. There may be symmetry-related attractors in these systems, and which attractor is approached may depend sensitively on the initial conditions. Dwell-time analysis is useful in this context because it allows to visualize in another way the repellers on the basin boundary which cause this sensitive dependence.

Introduction

Nonlinear dynamical systems with coexisting attractors are likely to produce fractal structures in the plane of initial conditions [1]. This also holds for 1-dimensional mappings. Here, the basin boundaries can be classified as being smooth, quasi-fractal or fractal [2].

An interesting special case are mappings obeying distinct symmetries. Due to the presence of the symmetry, attractors are either invariant under application of the symmetry operation, or there is a set of coexisting symmetry-breaking attractors which are transformed into each other by the operation. It has been demonstrated [3] that the structure of a basin boundary is determined by the mechanism of symmetry breaking in the latter case: for period-2 orbits with a broken symmetry the existence of the boundary gives rise to a quasi-fractal dependence of which attractor is eventually approached on initial conditions. This dependence is due to the existence of a repeller in phase space that allows a trajectory to escape into either of the coexisting attractors after performing a (sometimes very long) transient on the repeller. The behavior is reminiscent of chaotic scattering of particles due to a chaotic saddle in phase space [4]. The trajectories approach the saddle along the stable manifold, perform a transient, and finally leave along one of a few bundles of outgoing unstable manifolds. Similar to the present case the dependence of the outgoing states depends sensitively on initial conditions for these systems. This behavior is caused by the chaotic saddle. The mutual connection between properties of the saddle and sensitive dependence on initial conditions has successfully been uncovered by dwell-time analysis [5]. To the authors' knowledge, however, such an analysis has never been performed to analyse basin boundaries of coexisting attractors in one-dimensional maps.

In this paper we focus on the point that a fractal dependence on initial conditions is due to a repeller on the boundary of the basin of attraction of an attractor. Long transients into one of the attractors stay in the vicinity of the boundary for a long time. They provide information about this unstable set (cf. [6]), e.g. whether there are only a few unstable cycles or even a chaotic repeller on the basin boundary. Dwell-time plots form a useful tool in deciding this, because they allow to visualize the unstable sets.

2. Maps with Symmetry

Let us consider a d-modal [3, 7, 8] map

$$x_{n+1} = f(x_n, a), \quad f:[A_1, A_2] \to [A_1, A_2], \qquad (1)$$

where a is a control parameter and the function f on the interval on the real axis $[A_1, A_2]$ has a discrete symmetry s:

$$s \circ f = f \circ s, \quad s:[A_1, A_2] \to [A_1, A_2]. \qquad (2)$$

In the following we restrict us to the simplest case, namely to $s \circ s = 1$. The symmetry $s(x) = -x$ requires

* Paper presented at the 5th Annual Meeting of ENGADYN, Grenoble, October 10–13, 1994.

Reprint requests to Dr. J. Peinke.

0932-0784 / 95 / 1200-1117 $ 06.00 © – Verlag der Zeitschrift für Naturforschung, D-72027 Tübingen

that two kinds of M-cycles (M-periodic points) exist. On the one hand, there always are M-cycles, A, symmetric under s:

$$\{x^A_{*M}\} = s(\{x^A_{*M}\}), \tag{3}$$

where we have used the following notation for the M-cycle: $\{x^A_{*M}\} = \{x^A_1, \cdots, x^A_M\}$.

On the other hand, there may also be M-cycles, B, which are not symmetric under s. In that case there exists for each B another symmetry-conjugated M-cycle B' satisfying

$$s(\{x^B_{*M}\}) = \{x^{B'}_{*M}\}, \quad s(\{^{B'}_{*M}\}) = \{x^B_{*M}\}. \tag{4}$$

A discussion of the implications of the symmetry on the dynamics is given in [3], where they are illustrated by the map $f(x) = (1-a)\cdot x + a\cdot x^3$. This map is symmetric under inversion, i.e. it obeys the symmetry $s(x) = -x$. Our present discussion starts from these results. However, for the present paper we prefer to discuss the function

$$f(x) = (1-a)\cdot x + a\cdot x\cdot |x|, \tag{5}$$

which shows analogous behavior (Figure 1). It has the advantage to allow for analytical calculations of many of the parameter values of interest. In Fig. 2a the bifurcation diagram of (5) for one fixed initial condition is shown. There is only one stable fixed point $x^A_{*1} = 0$ for $a < 2$. At $a = 2$ there is a period-doubling bifurcation. At this bifurcation the fixed point becomes unstable, and a 2-cycle $x^A_{*2} = \{\pm\frac{a-2}{a}\}$ symmetric under s is born. It is stable for $2 < a < 4$. More interestingly, at $a = 4$, the symmetry of the attracting set in f is broken. The symmetric two cycle bifurcates, bringing forth two stable unsymmetric-2-cycles $\{x^B_{*2}\} = \{\frac{1}{2} + \sqrt{\frac{1}{4} - \frac{1}{a}},\ -\frac{1}{2} + \sqrt{\frac{1}{4} - \frac{1}{a}}\}$ and $\{x^{B'}_{*2}\} = \{\frac{1}{2} - \sqrt{\frac{1}{4} - \frac{1}{a}},\ -\frac{1}{2} - \sqrt{\frac{1}{4} - \frac{1}{a}}\}$, which are shown in Figure 1. Each of these orbits performs a period doubling cascade separately. During the whole cascade the symmetry of the map remains broken. It is only restored in a merging crisis [9] of the resulting chaotic bands which is clearly visible at $a \approx 4.679$. It is well known that there are no chaotic invariant sets in the map before the first period doubling cascade terminates [10]. In particular this implies that there cannot be a chaotic saddle on the basin boundary for $a \lesssim 4.6$. On the other hand, there certainly is a chaotic saddle in the period-4 window at $5.404 \lesssim a \lesssim 5.467$. Figure 2b shows a more detailed view of the bifurcation diagram on one of the four branches in this window. There is a symmetric period-4 cycle for $5.404 \lesssim a \lesssim 5.432$. Just as in the period-2 case this orbit bifurcates into two symmetry-broken period-4 cycles each of which performs a period-doubling cascade separately. Finally at $a \approx 5.455$ the symmetry is restored again.

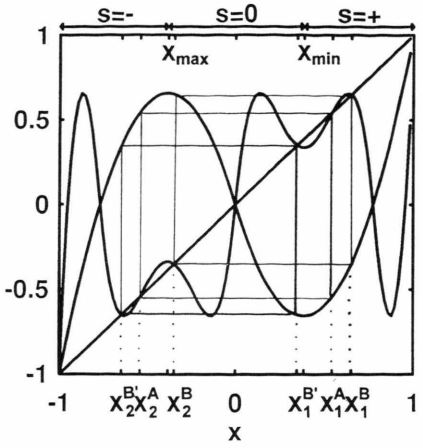

Fig. 1. Notations used in dealing with the map $f(x) = (1-a)\cdot x + a\cdot x\cdot|x|$. The map and its second iterate $f(f(x))$ are shown for the parameter value $a = 4.40$. For all parameter values the map has fixed points at -1, 0 and $+1$. For $a > 1$ the map also has a maximum and a minimum at $x_{max} = -\frac{a-1}{2a}$ and $x_{min} = \frac{a-1}{2a}$, respectively. At $a = 2$ a symmetric 2-cycle $\{x^A_{*2}\} = \{\pm\frac{a-2}{a}\}$ is born, which subsequently, at $a = 4$, gives rise to another two, symmetry-related 2-cycles $\{x^B_{*2}\} = \{\frac{1}{2} + \sqrt{\frac{1}{4} - \frac{1}{a}},\ -\frac{1}{2} + \sqrt{\frac{1}{4} - \frac{1}{a}}\}$ and $\{x^{B'}_{*2}\} = \{\frac{1}{2} - \sqrt{\frac{1}{4} - \frac{1}{a}},\ -\frac{1}{2} - \sqrt{\frac{1}{4} - \frac{1}{a}}\}$. The three intervals generating the symbolic encoding of trajectories are indicated by arrows on top of the figure.

The effect of symmetry breaking on the form of the basin boundaries will be discussed next. After symmetry breaking there are two coexisting attractors, thus there are two basins of attraction present. The structure of these basins are given by the closure of the stable manifold of unstable periodic points [2]. In [3] it was suggested to visualise the morphology of coexisting attractors and the unstable periodic points by plotting the values $x_N, \cdots, x_{N+M}$ as functions of the initial condition, where M is the periodicity of the attracting orbits and N is a number which has to be choosen sufficiently large to ensure that transients have died out for almost all initial values. In this way, quasi-fractal [2] behavior was found in the period-2 window. At the lower parts of Fig. 3 we present the corresponding plots for the map (5). At the parameter values taken in Fig. 3a the symmetric period-2 orbit

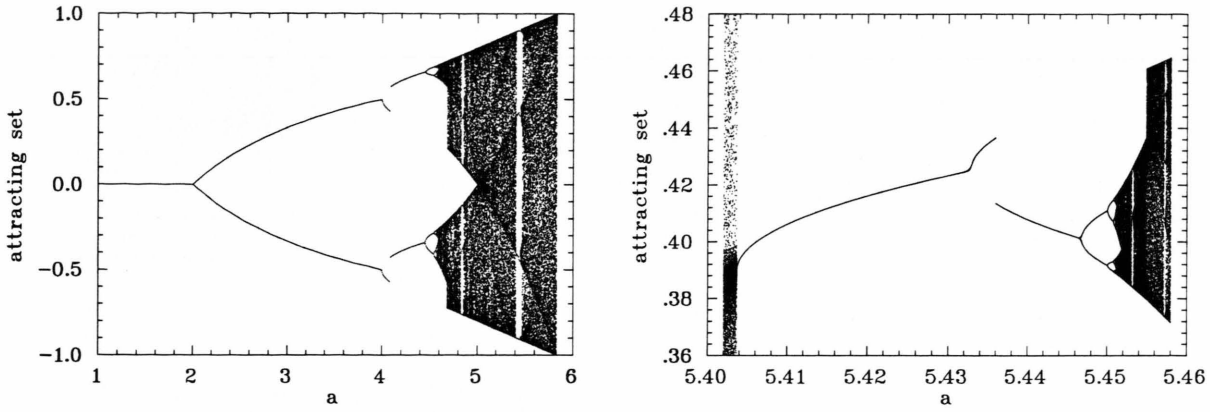

Fig. 2. Bifurcation diagrams for the map $f(x) = (1 - a) \cdot x + a \cdot x \cdot |x|$. (a) The map shows an attractor in the whole range from $a = 1$ till $a = 3 + \sqrt{8} \approx 5.8284$. There is an attracting fixed point at the former parameter value and a whole chaotic band at the latter one. For still larger values of a the attractor turns into a saddle, and almost all initial conditions escape to infinity. The values of a are chosen in steps of 0.02. For any of these values one initial point, $x = 0.01$, was iterated 250 times and the following 256 point are plotted. This gives a good description of the attracting set, because initial transients typically have died out after 250 iterations. Note that there are two symmetry-related attractors in the map for $4 < a \lesssim 4.679$. Due to the construction of the plot by one fixed initial condition, only one of them is shown in the plot. At $a \approx 4.1$ the initial condition changes the basin of attraction. As a consequence we jump from one attracting period-2 cycle to the symmetry-related one. (b) Detailed view of one of the branches in the period-4 window in the bifurcation diagram at $5.404 \lesssim a \lesssim 5.467$. The structure is very much the same as the one of the branches in the initial period-doubling cascade at $2 < a \lesssim 4.679$. At $a \approx 5.432$ the symmetric period-4 cycle bifurcates into two symmetry-related ones, which separately show period-doubling. For this plot a was increased in steps of 0.0001, and $x = 0.427$ was chosen as fixed initial point. The other parameters are kept the same as in (a). It was necessary to change the initial point for the iteration to ensure that the initial condition changes the basin of attraction only once (at $a \approx 5.436$). A typical initial condition, that is chosen outside the chaotic bands, changes the basin of attraction so frequently that the breaking of symmetry can no longer be discerned.

has not yet bifurcated into symmetry-broken orbits. The symmetric period-2 orbit is the only stable cycle, and almost all initial conditions approach this orbit. In Fig. 3b the corresponding plot is given for symmetry-broken period-2 orbits. In this case, there are two attracting orbits. As the orbits are symmetry related, half of the initial conditions are attracted to either one. As shown in Fig. 3c this dependence on initial conditions becomes much more complex in the period-4 window. The basins of attraction are intertwined to such a degree that they cannot be distinguished in these plots. In the vicinity of nearly all initial conditions belonging to one attractor there are points that approach the other attractor. This already indicates that the saddle on the boundary separating the basins of attraction has become fractal at these parameter values.

3. Analogy to Chaotic Scattering

For chaotic scattering [4] there is sensitive dependence of the final state on the incident impact parameter, which is well understood by now. It is due to a chaotic saddle in phase space which is commonly visualized by dwell-time plots [5]. A relation to these methods may be set up by regarding the asymptotic attractors in f as outgoing states for transients on the chaotic saddle: To define the dwell time one assigns a symbol sequence $\sigma_0 \sigma_1 \sigma_2 \sigma_3 \sigma_4 \cdots$ to every initial condition x_0 by setting

$$\sigma_i = \begin{cases} - & \text{for} \quad f^i(x_0) \in [-1, x_{\max}] \\ 0 & \text{for} \quad f^i(x_0) \in [x_{\max}, x_{\min}], \\ + & \text{for} \quad f^i(x_0) \in [x_{\min}, 1] \end{cases}$$

where $x_{\max}$ and $x_{\min}$ are the position of the maximum and the minimum of f given by $x = -\frac{a-1}{2a}$ and $x = \frac{a-1}{2a}$, respectively (cf. Figure 1). When the parameter a exceeds its critical value at the period-doubling bifurcation by a sufficient amount [11] the symmetric period-2 orbit corresponds to $\overline{-+}$, and the symmetry-broken orbits to $\overline{0+}$ and $\overline{0-}$, respectively. Note that the inversion symmetry also holds for this encoding: the orbit $\overline{-+}$ is invariant under multiplication of all symbols with -1, while $\overline{0+}$ and $\overline{0-}$ are mapped

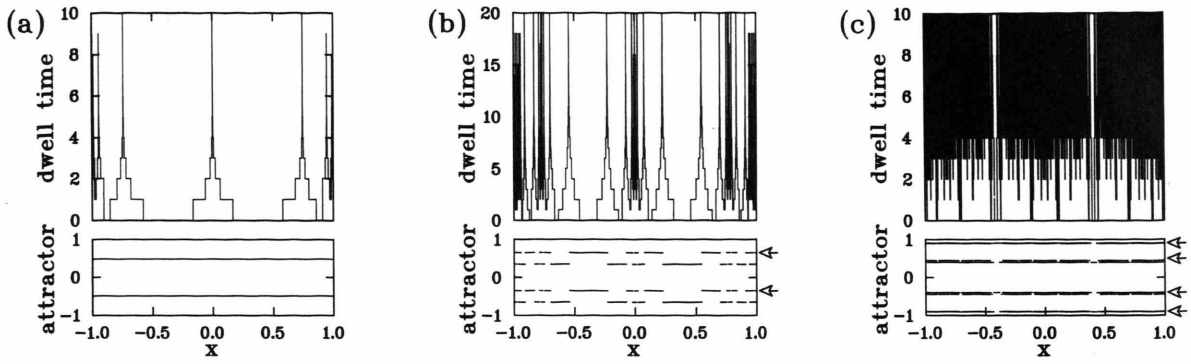

Fig. 3. Dwell-time plots are shown in the upper parts of the plots. To set up the connection with basin boundaries, the attractor an initial condition is heading to is shown in the lower part of the plots. The parameter values (a) $a = 3.9$, (b) $a = 4.40$ and (c) $a = 5.446$ are chosen for the respective plots. In (a) the symmetric period-2 cycles $\{x_{*2}^{A}\}$ is attracting. In (b) and (c), the symmetry is broken and there are symmetry-related attracting period-2 and period-4 cycles, respectively. The attracting 2-cycle $\{x_{*2}^{B}\}$ in part (b) has coordinates $\{0.65, -0.35\}$. It is indicated by arrows at the right-hand border of the lower plot. By symmetry, the other 2-cycle $\{x_{*2}^{B'}\}$ has coordinates $\{0.35, -0.65\}$. Similarly, one attracting period-4 cycle in part (c) is indicated by arrows. It has coordinates $\{0.4486, -0.8985, -0.4018, 0.9072\}$, while the symmetry-related one has coordinates $\{0.4018, -0.9072, -0.4486, 0.8985\}$. Only six lines can be distinguished in this plot, because the difference of the lines at ± 0.8985 and at ± 0.9072 is not resolved in the figure.

onto each other. A typical initial condition will give rise to a symbol sequence which after behaving non-periodic for a while, finally follows one of the attracting cycles. After all, at the beginning its position in the interval $[-1, 1]$ strongly depends on its initial conditions, while finally the point can hardly be distinguished from the stable cycle it is attracted to. One can easily remove the asymptotic periodic part from the initial aperiodic one. The number of symbols in the initial part represents the length of the transient until the attractor is approached. In the following this number will be called the *dwell time* of the transient starting in x_0. It is plotted in the dwell-time plots given in the upper parts of Figure 3. Points not being attracted to the stable cycles have an infinite dwell time. Their positions can easily be read off in the dwell-time plot although they are difficult to visualize otherwise, as they form a set of measure zero on the line of initial conditions. In particular, the form of the repeller on the basin boundary follows from these plots. When there is only a stable 2-cycle (Fig. 3 a) all points but the unstable fixed point in the origin and its pre-images approach the 2-cycle. There are no fractal or quasi-fractal sets, yet.

The structure of the dwell-time plot is much more interesting for the symmetry-broken orbits (Figure 3 b). Still, there are singularities at the fixed point $x = 0$ and its pre-images. Now, however, there is a multitude of additional singularities which correspond to the pre-images of the symmetric period-2 cycle. It is easily recognized that the symmetric 2-cycle separates the basins of attraction of the symmetry-broken 2-cycles. Therefore, its pre-images separate these domains, too: points in a sufficiently small neighborhood to the left and to the right of these pre-images approach different asymptotic states. This can be verified from the plot of the final state on initial conditions given in the lower part of the figure. The set of singularities in the dwell-time plot is already quite complicated for these parameter values. E.g. it is self-similar in the vicinity of the origin (Figure 4). The complexity of this set is the origin of the quasi-fractal dependence on initial conditions as it has been reported in [3]. However, the basin boundaries are not yet fractal at these parameter values. To that end a non-countable set of points with self-similarly organized neighborhoods has to be present while there are only countably many in this case, namely the one around the unstable fixed point at $x = 0$, and its pre-images. (Note that the pre-images of self-similar neighborhoods are self-similar themselves.) This can be inspected by comparison with Figure 3 a. The self-similar set of singularities around these points is due to a heteroclinic connections of the fixed point $x = 0$ and the symmetric period-2 cycle. The points on this orbit converge towards $x = 0$ under backward iteration. All of them give rise to a singularity in the dwell time, because they approach the (non-attracting) sym-

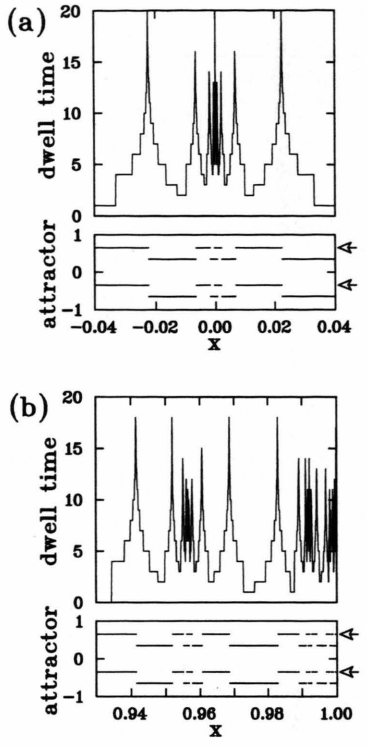

Fig. 4. At $a = 4.40$ the dwell-time plot shows a self-similar structure around the unstable fixed point $x = 0$ and its pre-images. The plot shows enlargements of the self-similar regions around (a) $x = 0$ and (b) to the left of $x = 1$, respectively. Note that, except for $x = \pm 1$, the self-similar structure is restricted to isolated points. Therefore the set of singularities is not a fractal.

metric period-2 cycle instead of one of the symmetry-broken ones under forward iteration. Analogously, the sets of singularities around the pre-images of $x = 0$ are given by "pree-images of the heteroclinic connection". (Keep in mind that the pre-images are not unique for the map (5).)

There also is a geometric approach to argue that the set of singularities in Fig. 3b is not fractal. To this end we look at the set $\mathscr{C}_n$ of initial conditions that have transients longer than n. This set is composed of M_n intervals. Most of these intervals do not split, but only shrink in size. Only the ones in the center of a self-similar neighborhood split into three under going from n to $n+1$: M_n grows quadratically in this case. For a fractal, on the other hand, the number of intervals has to grow exponentially. An example for such a behavior is shown in Figure 3c. It shows a dwell-time plot for the symmetry-broken period-4 cycles at $a = 5.42$. In that case almost all intervals split in every step $n \to n+1$ so that the number of intervals grows faster than 2^n. The set of singularities forms a fractal, and the corresponding saddle separating the basins of attraction of the two cycles shows chaotic behavior. The induced strongly chaotic behavior is the reason that one cannot identify intervals of initial conditions going to one of the symmetry-broken cycles when one starts outside the immediate vicinity of the attracting orbits. For most initial conditions the attracting set shown at the lower part of Fig. 3c looks like an 8-cycle. However, from the numerical data one sees that there are actually two 4-cycles, and that the initial conditions change on an extremely fine scale between these two.

4. Summary

In this paper we have studied the basin of attraction of symmetry-related periodic attractors in a one-dimensional model. We have pointed out that the sensitive dependence of the final state (i.e. the attractor approached) on the initial conditions is caused by a repeller on the basin boundary. Dwell-time plots [5] have been used to visualize repellers in the context of chaotic scattering [4]. Adoption of this technique for the present problem allows to distinguish smooth, quasi-fractal and fractal behavior by visual inspection. This is an advantage compared to approaches in the literature that rely on testing the accessibility of boundary points from the interior of basins of attraction [2], or on plotting the final state as function of initial conditions [3]: the former approach is laborious, in general, while the latter one gives less information on the structure of the repeller. A combination of the latter approach and dwell-time analysis, however, provides an efficient numerical tool allowing for a straightforward inspection of the repeller and the related fractal or quasi-fractal behavior. Moreover, this approach is interesting from a conceptual point of view because it relates concepts introduced to study the structure of basin boundaries in systems with multiple attractors with concepts of transient chaos.

Acknowledgements

This paper was prepared for the Proceedings of the ENGADYN-Herbsttreffen, Le-Cucheron, October 9–13, 1994. The authors thank all participants for the pleasant atmosphere and many lively discussions during the workshop. In particular they are indebted to A. Kittel for suggestions and discussions. J. V. acknowledges financial support by the Schweizerischer Nationalfonds, and J. P. a Heisenberg fellowship by the Deutsche Forschungsgemeinschaft.

[1] B. B. Mandelbrot, The Fractal Geometry of Nature, Freeman, New York 1982; H.-O. Peitgen, H. Jürgens, and D. Saupe, Chaos and Fractals, Springer-Verlag, New York 1992.

[2] L. Kocarev, Phys. Lett. **A 121,** 274 (1987); **A 125,** 389 (1987).

[3] A. Okniński, R. Rynio, and J. Peinke, Chaos, Solitons, and Fractals **5,** 783 (1995).

[4] B. Eckardt, Physica **D 33,** 89 (1988); U. Smilansky, in M.-J. Giannoni, et al. ed.: Chaos and Quantum Physics, Les Houches, Session LII, 1989, Elsevier, Amsterdam 1992; E. Ott and T. Tél, Chaos **3,** 417 (1993).

[5] D. W. Noid, J. Chem. Phys. **84,** 2649 (1986); B. Eckhardt and C. Jung, J. Phys. A: Math. Gen. **19,** L829 (1986); P. Gaspard and S. A. Rice, J. Chem. Phys. **90,** 2225 (1989); S. Bleher, C. Grebogi, and E. Ott, Physica **D 46,** 87 (1990); Z. Kovaćs and T. Tél, Phys. Rev. Lett. **64,** 1617 (1990).

[6] I. M. Janosi, L. Flepp, and T. Tél, Phys. Rev. Lett. **73,** 529 (1994); I. M. Janosi and T. Tél, Phys. Rev. **E 49,** 2756 (1994).

[7] M. Yu Lyubich, Ergod. Th. and Dynam. Sys. **9,** 737 (1989).

[8] W. de Melo and S. van Strien, One-dimensional dynamics, Ergebnisse Series, Springer, Berlin 1993.

[9] C. Grebogi, E. Ott, and J. A. Yorke, Phys. Rev. Lett. **48,** 1507 (1982); C. Grebogi, E. Ott, and J. A. Yorke, Phys. Rev. **A 36,** 5365 (1987); E. Ott, Chaos in Dynamical Systems, Cambridge Univ. Press, Cambridge 1993.

[10] S. Grossmann and S. Thomae, Z. Naturforsch **32 a,** 1353 (1977); J.-P. Eckmann and D. Ruelle, Rev. Mod. Phys. **57,** 617 (1985).

[11] More precisely, a has to be chosen beyond the value where the newly created symmetry-broken cycles are superstable. Otherwise, they cannot be distinguished from the symmetric one.